This pdf circulated in Volume 4, Number 25, on 5 March 2012.

Space Environmental Viewing and Analysis Network (SEVAN) – characteristics and first operation results

A. Chilingarian, K. Arakelyan, K. Avakyan, N.Bostanjyan, S. Chilingaryan, V. Danielyan, G.Hovsepyan, T. Karapetyan, L.Kozliner, B. Mailyan, D. Pokhsraryan, A. Reymers, D. Sargsyan, M. Zazyan

Yerevan Physics Institute,
Alikhanyan Brothers 2, Yerevan 375036, Armenia

Abstract

Space Environmental Viewing and Analysis Network (SEVAN, A.Chilingarian&Reimers, 2008, A.Chilingarian et al., 2009, S.Chilingarian et al., 2009, Roša et al, 2010) is a worldwide network of identical particle detectors located at middle and low latitudes aimed to improve fundamental research of space weather conditions and to provide short- and long-term forecasts of the dangerous consequences of space storms. SEVAN detected changing fluxes of different species of secondary cosmic rays at different altitudes and latitudes, thus turning SEVAN into a powerful integrated device used to explore solar modulation effects. Till to now the SEVAN modules are installed at Aragats Space Environmental Centre in Armenia (3 units at altitudes 800, 2000 and 3200 m a.s.l.), Bulgaria (Moussala), Croatia and India (New-Delhi JNU.) and now under installation in Slovakia, LomnitskySchtit). Recently SEVAN detectors were used for research of new high-energy phenomena originated in terrestrial atmosphere – Thunderstorm Ground Enhancements (TGEs, Chilingarian et al., 2010, 2011). In 2011 first joint measurements of solar modulation effects were detected by SEVAN network, now under analysis.

1. Introduction

The sun influences Earth in different ways by emissions of electromagnetic radiation, interplanetary plasma structures and high-energy particles. Although the entire energy of the high- energy particles comprises very small fraction of the visible light energy, nonetheless the study of these particles gives clues about fundamental and universal processes of particle acceleration and their interactions with interplanetary magnetic field; thus providing information about the consequences of the huge solar explosions affecting the near-Earth environment, space born and surface technologies, i.e. so-called space

weather issues. During billions of years of its evolution, the Earth was bombarded by the protons and fully stripped ions accelerated in the Galaxy during tremendous explosions of the supernovae and by other exotic stellar sources. This flux was may change on the passage of the sun through the four galactic arms during its path around the center of Galaxy and was affected several times by huge explosions of nearby stars. Nonetheless, on the shorter time scales the intensity of the Galactic Cosmic Rays (GCRs) is rather stable. In turn, our nearest star – the sun is a tremendously variable object, capable of changing radiation and fluxes of the Solar Cosmic Rays (SCR) by 3–4 orders of magnitude in the span of a few minutes. These transient events are called Solar Energetic Proton events (SEPs). Because of the sun's closeness, the effects of the changing fluxes have major influence on Earth, including climate, safety and other issues. The influence of sun on the near-Earth radiation environments can be described as modulation of the stable galactic cosmic ray ''background'' by the sun activity. The sun ''modulates'' the low energy GCR in several ways. The most energetic flaring process in the solar system releases up to 10^{33} erg of energy during few minutes. Along with broadband electromagnetic radiation, the explosive flaring process usually results in the Coronal Mass Ejection (CME) and in acceleration of the copious electrons and ions. Particles can be generated either directly in the coronal flare site with subsequent escape into interplanetary space, or they can be accelerated in CME associated shocks that propagate through corona and interplanetary space. These particles are effectively registered by the particle spectrometers on board of space stations (SOHO, ACE) and satellites (GOES, SDO). However, the direct measurement of highest energy SCR (above 1 GeV/nucleon) by space-born facilities is not feasible yet due to payload and time-of-flight limitations. Highest energy SCRs generates particle showers in interactions with atmosphere nuclei that can reach the Earth and generate additional (to ones initiated by GCR) signals in surface particle detectors. Therefore, surface particle detectors measure energetic SEP events also. This phenomenon is called Ground level enhancement (GLE). The latitudinal dependence of the geomagnetic field provides the possibility to use the dispersed worldwide network of Neutron Monitors (NM, Moraal, 2000) as a spectrometer registering GCR in the energy range from 0.5 to 10 GeV.

The spectra of GCR and SCR can be approximated by the power law $dJ/dE \sim E^{\gamma}$, for the GCR $\gamma \sim -2.7$. SCR flux at GeV energies usually is very weak ($\gamma > 6$), only at some events, such as at 23 February 1956 or 20 January 2005, the spectra of SCR are considerably ''hard'': $\gamma \sim -4$ - -5 at highest energies. Thus, for energies greater than 10 GeV the intensity of the GCR becomes increasingly higher than the intensity of the largest known SEP events and we confront a very complicated problem of detecting a small signal of the SCR against the huge ''background'' of the GCR. Existing networks of particle detectors are unable to reliably detect very low fluxes of the SCR above 10 GeV; low statistics experiments often demonstrate fake peaks with high significances[1]. Therefore, the maximal energy E_{max} of solar accelerators is still not determined. Recent measurements at Aragats Space-Environmental Center (ASEC, Chilingarian, 2003, 2005) based on the huge SEP of January 2005 put the maximal energy of solar accelerators up to 20 GeV (Bostanjyan & Chilingarian, 2008, Chilingarian & Bostanjyan, 2009).

Preceding from measured enhanced secondary fluxes of the different charged and neutral particles at earth surface it is possible to estimate the energy spectra power law index of the SEP

[1]Some remedies to avoid erroneous inference on existence of a signal were discussed in (Chilingarian, 2009).

event. The estimated index of γ = -4 - -5 at GeV energies is a very good indicator for the severe radiation storm (abundant SCR protons and ions with energies 50 - 100 MeV, see Chilingarian & Reymers, 2007), extremely dangerous for the astronauts and high over-polar flights, as well as for satellite electronics. Each of the measured secondary fluxes has a different most probable energy of primary "parent" proton/nuclei. As we demonstrate in (Zazyan & Chilingarian, 2009), for the Aragats facilities these energies vary from 7 (most probable energy of primary protons generated neutrons) to 20-40 GeV (dependent on the spectra; index of SCR, most probable energy of primary protons generating muons with energies greater than 5 GeV). Thus, for predicting upcoming radiation storm it is necessary to monitor changing fluxes of the different species of secondary cosmic rays with various energy thresholds. To cover wide range of SCR energies we need networks of particle detector at different latitudes longitudes and altitudes.

Other solar modulation effects also influence the intensity of the cosmic rays in the vicinity of Earth. Huge magnetized plasma structures usually headed by shock waves travel in the interplanetary space with velocities up to 3000 km/s (so-called interplanetary coronal mass ejection - ICME) and disturb the interplanetary IMF and magnetosphere. These disturbances lead to major geomagnetic storms harming multibillion assets in space; in the same time these disturbances introduce anisotropy in the GCR flux making depletion and enhancement regions manifested themselves as anisotropic distribution of GCR. Thus, time series of intensities of high-energy particles can provide highly cost-effective information also for the forecasting of the geomagnetic storm (Leerungnavarat et al., 2003). With data from networks of particle detectors we can estimate the GCR energy range affected by ICME and reveal the energy-dependent pattern of the ICME modulation effects, namely Forbush decreases (FD, see Bostanjyan, Chilingarian, 2009), are the attenuations of the GCR flux in the course of a few hours with following recovering during several days. Measurements of the FD magnitude in the fluxes of different secondary CR species reveal important correlations with the speed, size of the ICME and the "frozen" in ICME magnetic field strength (Chilingarian and Bostanjyan, 2010). Measurements of all the secondary fluxes at one and the same location are preferable due to effects of the longitudinal dependence of the FD magnitudes (Haurwitz et al., 1965). The research of the diurnal variations of GCR in fluxes of charged and neutral secondary CR also opens possibilities to correlate the changes of parameters of daily wave (amplitude, phase, maximal limiting rigidity) with energy of GCRs (Mailyan and Chilingarian, 2010).

Thus, for the basic research of solar physics and solar-terrestrial connections and Space weather, as well as for establishing services of alerting and forecasting of dangerous consequences of space storm the networks of particle detectors located at different geographical coordinates and measuring various species of secondary cosmic rays are of vital importance.

A network of particle detectors located at middle to low latitudes known as SEVAN (Space Environment Viewing and Analysis Network, Chilingarian &Reymers, 2008, Chilingarian et al., 2009) was developed in the framework of the International Heliophysical Year (IHY-2007) and now operates and continue growth within International Space Weather Initiative (ISWI). SEVAN detectors measure time series of charged and neutral secondary particles born in cascades originating in the atmosphere by nuclear interactions of protons and nuclei accelerated in the Galaxy and nearby the sun. The SEVAN network is compatible with the currently operating high-latitude neutron monitor networks ''Spaceship Earth'' (Kuwabara et al. 2006), coordinated by the Bartol Research Center, the Solar Neutron Telescopes (SNT) network coordinated by

Nagoya University (Tsuchiya et al. 2001), the Global Muon Detector Network (GMDN) (Munakata et al. 2000, Rockenbach et al., 2011), the Eurasian Neutron Monitor Data Base (Mavromichalaki et al. 2005, 2006) and a new muon–neutron telescope constructed at Yangbajing, Tibet, China (Zhang et al., 2010).

SEVAN modules are operating in Armenia (4 one m^2 standard modules and 2 super modules of 12 identical SEVAN units each arranged above and below 2 standard sections of Nor Amberd neutron monitor 6NM-64; both super modules are capable of muon direction estimation), in Croatia (Zagreb observatory), Bulgaria (Mt. Moussala, India (New-Delhi JNU Univ.) and are under construction in Slovakia (Mt. Lomnicky Stit).

The potential recipients of SEVAN modules are Israel, Germany and Costa Rica (Figure 1). The analogical detector is in operation in Tibet (China, Zhang et al., 2010).

Figure 1.SEVAN network; World map with operated and planned particle detectors.

SEVAN network provides reliable monitoring of the Sun by ~16 h per day.

The particle fluxes measured by the new network at medium to low latitudes, combined with information from satellites and particle detector networks at high latitudes, will provide experimental evidence on the most energetic processes in the solar system and will constitute an important element of the global space weather monitoring and forecasting service. In the paper we present the description of SEVAN modules, its possibility to measure charged and neutral fluxes; excepted purities and efficiencies of secondary cosmic ray registration, as well as the first results of the SEVAN network operation. Also we demonstrate the ability to measure energy spectra of the solar protons by registering the GLEs; possibilities to distinguish between neutron-

and proton-initiated ground level events (GLEs), and some other important properties of hybrid particle detectors. Separate chapter is devoted to registration of the Thunderstorm ground enhancements, new high-energy phenomena in the atmosphere. SEVAN modules, operated at slopes of Mt. Aragats in Armenia during recent years detect many TGE events in fluxes of gamma rays and high-energy muons, proving existence of the strong electrical fields in the thunderclouds initiating relativistic runaway electron avalanches in the thunderstorm atmospheres (Chilingarian et al., 2010, 2011). SEVAN detectors was calibrated by the gamma ray flux of the most powerful TGEs and furthermore, the time series of the high energy muons detected by SEVAN open possibility to estimate the electrical structure of the thunderclouds, the key parameter for creating models of both TGE and lightning occurrences.

2. Design of SEVAN Particle Detectors

The basic detecting unit of the SEVAN network (see Figure 2) is assembled from standard slabs of 50 x 50 x 5 cm^3 plastic scintillators. Between two identical assemblies of 100 x 100 x 5 cm^3 scintillators (four standard slabs) are located two 100 x 100 x 5 cm^3 lead absorbers and thick 50 x 50 x 25 cm^3 scintillator assembly (5 standard slabs). A scintillator light capture cone and photo multiplier tube (PMT) are located on the top, bottom and the intermediate layers of detector. The detailed detector charts with all sizes are available from http://aragats.am/SEVAN.

Incoming neutral particles undergo nuclear reactions in the thick 25 cm plastic scintillator and produce protons and other charged particles. In the upper 5 cm thick scintillator charged particles are registered very effectively; however for the nuclear interactions of neutral particles there is not enough matter. When a neutral particle traverses the top thin (5 cm) scintillator, usually no signal is produced. The absence of the signal in the upper scintillators, coinciding with the signal in the middle scintillator, points to neutral particle detection. The coincidence of signals from the top and bottom scintillators indicates the traversal of high-energy muons. Lead absorbers improve the efficiency of the neutral flux detection and filtered low energy charged particles.

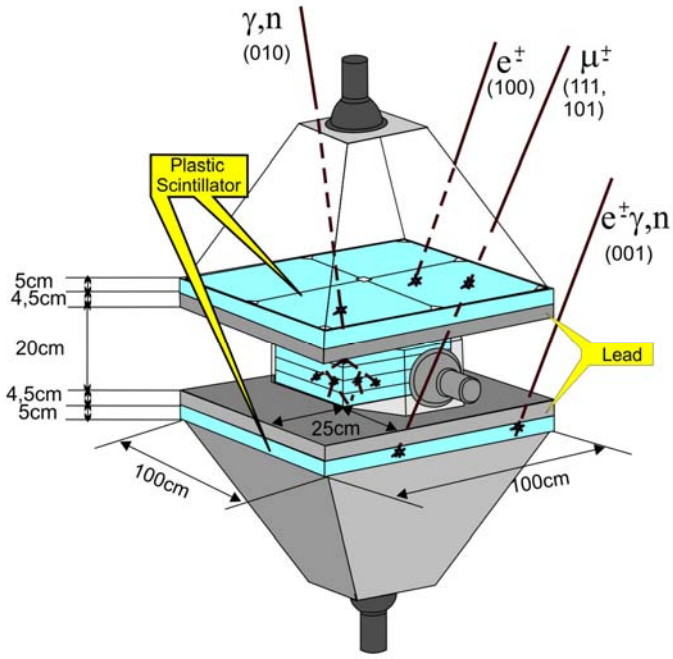

Figure 2.Basic detecting unit of the SEVAN network.

If we denote by ‘‘1’’ the signal from a scintillator and by ‘‘0’’ the absence of a signal, then the following combinations of the 3-layered detector output are possible:

111 and 101—traversal of high energy muon; 010—traversal of a neutral particle;100—traversal of a low energy charged particle stopped in the scintillator or in the first lead absorber (energy less than *100 MeV).110—traversal of a higher energy charged particle stopped in the second lead absorber. 001—registration of inclined charged particles

Microcontroller-based Data Acquisition SEVAN DAQ Electronics

Data Acquisition electronics consists of 8-Channel Discriminator/Counter Unit (8DCU) and 3 High Voltage supplies with presetting and automatic control, which are located in the corresponding PMT cases (Figure 3).

8DCU consists of:

- The 8-channel Programmable Threshold Comparator and Counter board (8CNT).
- Universal RS232/RS485 interface/power supply module - IFCC, Power transformer - 220V50Hz to 2x8V 0.5A + 2x15V 1.25A

Figure 3.SEVAN DAQ module.

The main features used in 8DCU are:

- 8 programmable threshold analog input (BNC connectors),
- Threshold programming range 4mV-1000mV with 4mV step,
- Powered by AC 50-60Hz 220V, 30W,
- Maximal counting frequency – 60kHz,
- LEDs to indicate the input pulses in each of 8channels, module power and programmable trigger condition.

8CNT board is used as a standalone 8-channel counter with a programmable threshold. For the threshold programming and the output data readout, it can communicate with the host PC (local network) through the IFCC module by any of RS-232 or RS-485 interface ports. The module counter and interface logic is based on the Atmel AVR Atmega88 (Atmel Corporation, 2008) 8-bit microcontroller. The same ATNGW100 Network Gateway Kit equipped with AVR32 Digital Signal Processor CPU is used as on-line PC for SEVAN modules. The ATNGW100 is equipped with 32 MB SDRAM, 8 MB data flash and 2 GB SD flash memory (see Figure 4). The communication is feasible through two Ethernet ports, UART, USB, and JTAG. The external storage can be connected using SD and MMC card reader. The FPGAs are programmed to realize 60 asynchrony counters to the serial port. In the preloaded LINUX system the serial ports are attached to /dev/ttyS1 и /dev/ttyS2. The system console port is attached to /dev/ttyS0. To provide access to third serial port we have recompiled a LINUX kernel. The port parameters are 8/n/1 115200 b/c.
Each second the counts accumulated in counters are transferred to ATNGW100 and are stored in hexadecimal format in 120 bite portions. Once a minute the data are archived to the /media directory which reside on the mounted flash card. If the flash card is not installed, the /media directory is mounted to the embedded flash memory. The NTP client installed on

NGW performs the time synchronization. FTP server is configured to serve the data to data acquisition software. Remote control is enabled by means of SSH and Telnet servers.
The data transfer software twice a second read out serial ports buffers and integrate it up to 1 minute. Then 1- minute data are transferred to ATNGW100 in 120 bit portions and are stored in hexadecimal format. The number of blocks is checked and in the case if it's not equal to 60 (number of seconds in a minute) the minute count is proportionally scaled.

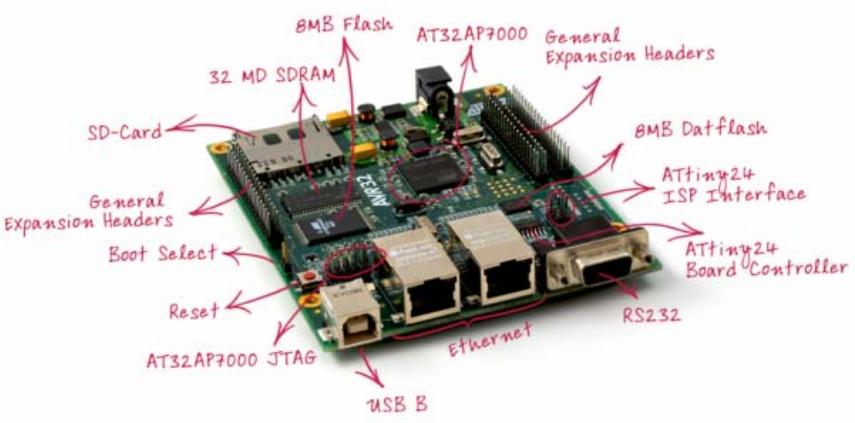

Figure 4.ATNGW100 Network Gateway Kit.

DAQ software consists of the host PC program and the microcontroller program (firmware). The firmware for the DAQ and control is written in C language and stored in the microcontroller reprogrammable flash memory. Below is presented the functionality, implemented for the SEVAN detector setup. In this case the microcontroller operates both for the thresholds presetting and control and as a main DAQ controller, with listed below functions:

- Counting of signals in each of 8 channels,
- Counting of all types of coincidences of signals in channels 1-3.

The gate for the coincidences registration is in the range 0.875 μsec. The dead time of the counters is 8 μsec. The maximal frequency of operation is 62 kHz that meets expected data rate at all possible SEVAN locations. The data collection time is set by the microcontroller firmware, so any other value can be chosen. The IFCC interface module has three connections: to the microcontroller, to the RS232 connector (DSUB9F) and RS485 connector (DSUB9M). The signals propagate from each of the mentioned connections to both of others. The power for the PMT High Voltage supplies (15V unregulated, 1.2Amax) is supplied from the 8DCU through the RS485 interface connector. The counters' contents are sent out via RS232 or/and RS485 interfaces each second in the format:

Cnt1 Cnt2 Cnt3 Cnt4 Cnt5 Cnt6 Cnt7 Cnt8

Co12 Co13 Co23 Co123

<blank line>

whereCntX – is the count of pulses in channel X in 1 second, CoXY(Z) – is the count of coincidences in channels X, Y. For example, Co12 is a number of coincidences in channels 1 and 2, without signals in channel 3.

Programmable Regulated High Voltage DC Power Supply (PRHVPS)

The Programmable Regulated High Voltage DC Power Supply is designed to supply high voltage to different electrodes on photomultipliers and various elementary particle detectors (Figure 5).

Industrial DC-DC power supplies usually need for the remote control ADC-equipped cards (Pulse Power & Measurement Ltd, 2008). Our solution consists in high voltage power supply with build in controlled via serial interface RS-485. Using the ATNGW100 Network Gateway Kit it is possible to remote tuning of the thresholds of discriminators and high voltage values for detector channels via Ethernet port.

The PRHVPS consists of:

- Current-driven, low-noise sine wave DC/DC converter, with up to 2 stage RC output ripple
- Pulse Width Modulated programmable DC regulator
- Local +5V linear voltage regulator
- Atmel microcontroller
- RS485 interface chip
- Optional temperature sensor

The Printed Circuit Board (PCB) can be assembled with various options for different output polarity, programmable voltage range, and so on.

Specific Features:

- Voltage programming in two hardware selectable ranges ± 900V to 2100V and ±1500 to 3000V in 2V steps
- Output voltage ripple less than 1mV
- Max. output current 1.2 mA for ± 900V to 2100V range; 0.8 mA for ±1500 to 3000V range
- Input voltage from +12V to +15V
- Absolute output voltage regulated to accuracy ±1V
- Optional temperature sensor
- RS-485 half-duplex 2-wire 9600 baud interface for programming and monitoring the output voltage

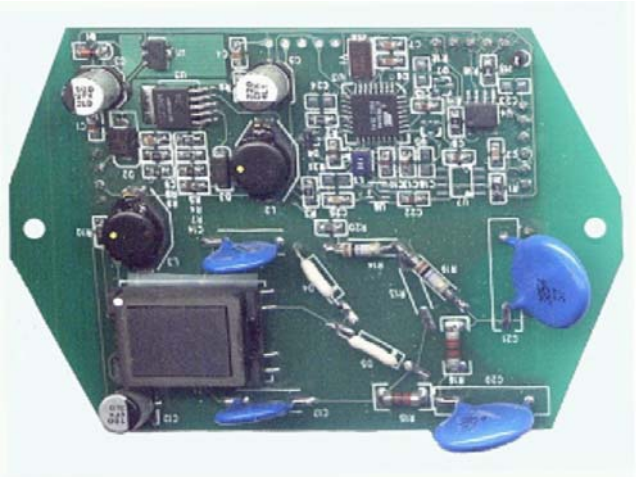

Figure 5. Programmable Regulated High Voltage DC Power Supply.

After one year operation of most components of the ASEC DAQ it proves reliability and multifunctional possibilities. Several papers are published based on the new physical results enabled by flexible and powerful DAQ system.

3. Characteristics of secondary cosmic ray fluxes detected by SEVAN modules

The modules of the SEVAN network located on different latitudes, longitudes and altitudes are probing different populations of primary cosmic rays. The SEVAN modules measure fluxes of neutrons and gammas, of low energy charged particles and high-energy muons. To understand the response of the new network to SEP events we calculate using CORSIKA code (Heck et al., 1998) most probable energies of primary protons to which the SEVAN modules, located at

different latitudes, longitudes and altitudes are sensitive (Zazyan& Chilingarian, 2009, see Table 1). The calculations were made for different values of the spectral index of the power low energy spectrum of the primary cosmic ray: for the GCRs (γ = -2.7); for the SEP events (γ = -4, -5, and -6). From the table we can see that SEVAN network provides registration of the SEP events in broad energy range included very poorly researched energies above 10 GeV. For instance, neutron fluxes measured at Lomnisky Stit, Slovakia are sensitive to 4 GeV solar protons and high energy muon flux measured at Delhi is sensitive to 18 MeV solar protons. Taking into account intermediate energies measure at Aragats, Armenia, Zagreb ,Croatia and Moussala, Bulgaria we can reliably recover SEP energy spectrum with unprecedented accuracy.

Table 1.The range of most probable energies (in GeV) of primary protons producing secondary fluxes at different SEVAN sites.

Station	GCR (γ=2.7)				SCR (γ=4,5,6)			
	Charged particles	Muons(E > 250 MeV)	Muons (E > 5 GeV)	Neutron	Charge particle	Muons (E > 250 MeV)	Muons (E > 5 GeV)	Neutron
Yerevan (Armenia)	14.6	18.4	38.4	7.1	8.2–1.2	10–11.6	21.2 - 31.9	7.1
Nor-Amberd (Armenia)	13.1	14.9	41.2	7.1	7.6–10.6	9.7–11.3	20.5–31.3	7.1
Aragats (Armenia)	10.9	14.3	37	7.1	7.4–10	7.6–10.6	21.2–27	7.1
Moussala (Bulgaria)	10.6	13.3	–	7.4	6.6–7.4	7.1–9.5	–	7.6–9.4
Zagreb (Croatia)	17.4	17.3	–	7.6	9.4–12.9	9.1–13.4	–	5.1–5.7
Lomnisky Stit (Slovakia)	11.5	14.5	–	4.1	4.1 −6.5	5.2–8.3	–	4
Delhi JNU (India)	18.1	18.1	–	16.5	14.2–15.1	14.3–15.3	–	14.3–14.4

To quantify statements about the detection of different types of particles by the SEVAN modules, we need to perform detailed simulation of the detector response. We use simulated cascades of the charged and neutral secondary particles obtained with the CORSIKA (version 6.204) Monte Carlo code (Heck et al., 1998). All secondary particles were tracked until their energy dropped below the predetermined value (50 MeV for hadrons, 10 MeV for muons and 6 MeV for electrons and photons) or reached all the way to the ground level. The spectra of primary protons and helium nuclei (99% of the flux at energies up to 100 GeV) are selected to follow the proton and helium spectra reported by the CAPRICE98 balloon-borne experiment (Boezio et al., 2003). Among the different species of secondary particles, generated in nuclear-electromagnetic cascades in the atmosphere, muons, electrons, γ-rays, neutrons, protons, pions and kaons were followed by CORSIKA and stored. These particles were used as input for the GEANT3 package (GEANT, 1993), implemented for detector response simulation. Also, we take into account the light absorption in the scintillator (Chilingarian et al., 2007). The efficiency of the charged particle detection by all 3 layers of the SEVAN detector is above 95%; the neutron detection efficiency in the middle "thick" scintillator reaches 30% at 200 MeV, the efficiency of the γ-quanta detection reaches 60% at the same energies. The purity (relative fraction of different species registered) of 3 SEVAN detecting layers is presented in Figure 6.

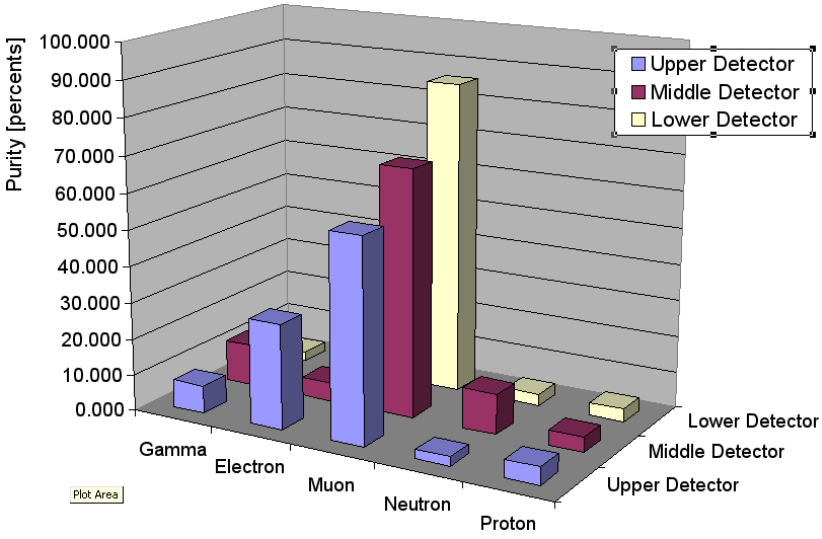

Figure 6. The purity of 3 SEVAN layers.

In Figure 6 we see that majority of registered particles in all 3 layers are muons; the first layer also is registering electrons. The fraction of neutral particles is uppermost in the middle layer, although it is less than 10% there. It is apparent that using only layer counts we will not be able to research the modulation effects the sun pose on different species of secondary cosmic rays; we should "enrich" the detected fluxes by the particles of definite types. The coincidence techniques described in previous sections allows us to perform this task by registering different combination of signals in the 3-layered detector. In Figure 7 we post the fraction of different particles registered by various combinations of the SEVAN module layers operation. The pattern is

significantly improved: fraction of electrons in events selected by combination 100 is above 40%; fraction of neutral particles selected by combination 010 – is larger than 85% and fraction of high energy muons in events selected by combinations 111 and 101 reaches 95%. Therefore, by analyzing combinations, instead of layer counts we can get clues how 3 types of secondary cosmic rays are influenced by meteorological and solar modulation effects. The data from Figures 6 and 7 are summarized in Table 2. The figures show that different layers are sensitive to different particles.

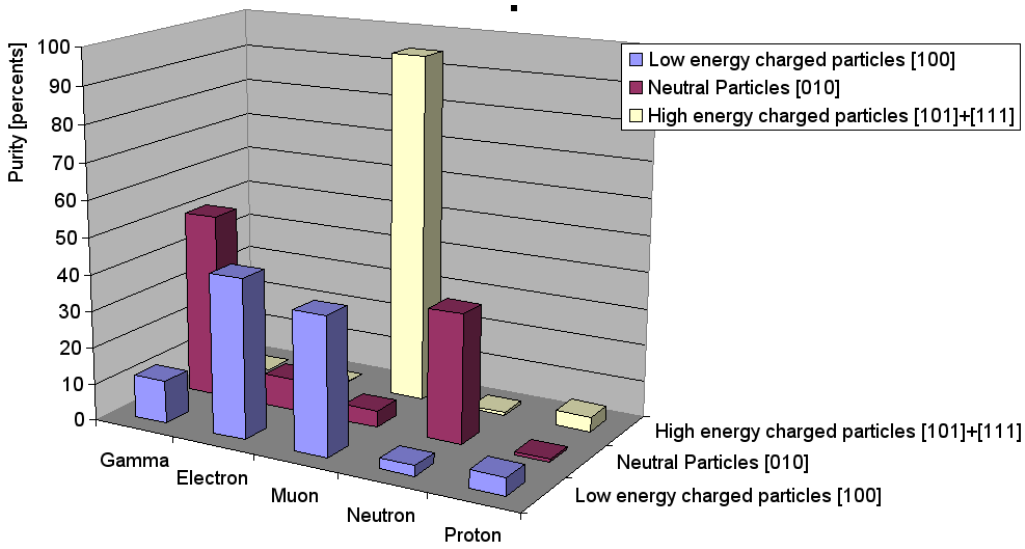

Figure 7.Purity of SEVAN combinations.

Table 2.Summary of particle selection purity by SEVAN layers and combinations.

	Gamma	Electron	Muon	Neutron	Proton
Registered particles Purity by special combination					
Low energy charged particles [100]	11.605	43.300	37.380	2.838	4.804
Neutral Particles [010]	50.612	8.837	4.494	35.071	0.972
High energy charged particles [101]+ [111]	0.002	0.106	94.904	0.808	4.077
Registered particles Purity by count rate of the detectors					
Upper Detector	7.616	28.952	56.080	2.448	4.814
Middle Detector	11.550	5.223	67.913	11.038	4.167
Lower Detector	2.696	4.438	85.873	3.267	3.634

Of course, the purity is not only parameter we are interested in; the efficiency of particle registration is also of upmost interest in detector design and operation. In Figure 8 we post the purity-efficiency diagram explaining which fraction of primary flux will contribute to different combinations.

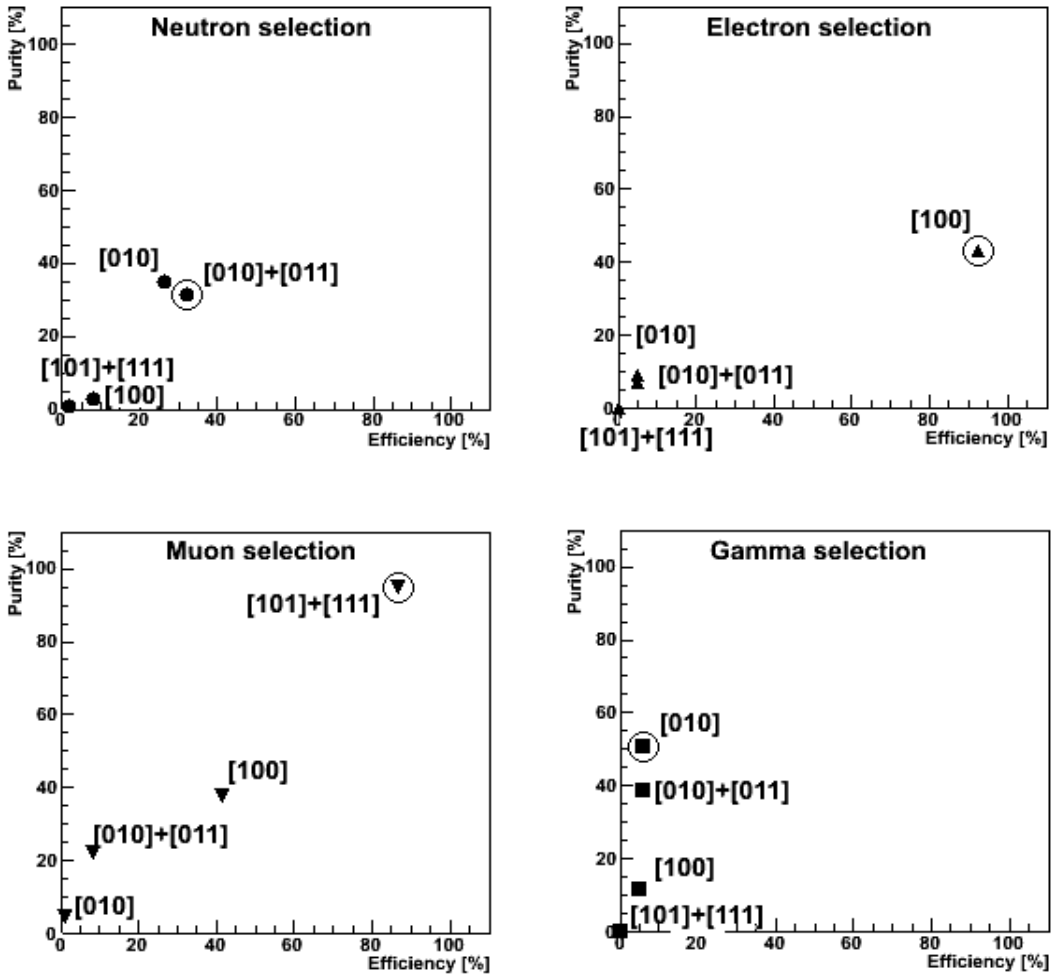

Figure 8. The purity-efficiency diagram of the SEVAN combinations registering ambient population of the secondary cosmic rays generated by interactions of GCR with atmosphere.

In Figure 8 we see that the high-energy muons are registered with both high efficiency and purity. Neutrons are registered with rather high efficiency and purity (both ~30%). It is worth to mention that efficiency of neutron monitor is reaching 30% only for highest energy neutrons. However NM can distinguish neutrons from the gamma rays (NM has excellent purity to select primary hadrons). Gamma rays are selected with lower efficiency by all possible combinations of SEVAN layers; nonetheless efficiency of electron registration is above 90%; therefore, the low energy electromagnetic component is registered efficiently by SEVAN.

For the particles registered by SEVAN we can obtain from simulation the most probable energies of primary GCR responsible for their origination. In Table 3 we post the most probable energies (medians of the energy distribution of the parent protons) producing different elementary particles in the terrestrial atmosphere. From the table we can see that the higher energy protons produce secondary muons and electrons compared with ones producing secondary neutrons.

Table 3. Modes of the GCR energy spectra corresponding to different species of secondary particles registered by the SEVAN detector at 3200 m above sea level.

Layers of detector located at 3200 m	Most probable energy of GCR (GeV)
Upper Layer	11.5
Middle 25 cm layer	8.5
Bottom Layer	14.5

As we can see in Table 2 and in Figure 8, SEVAN can register the low energy charged component, neutral component and high-energy muons. In Table 4 we compare the simulated and measured one-minute count rates of these particles. Low energy charged particles, as well as neutrons and gamma rays, are attenuated very fast as they penetrate deep in atmosphere. High-energy muons did not attenuate so fast as one can see in third row of Table 4.

Table 4.Experimental and simulated one-minute count rates measured by three scintillators of the SEVAN.

	Yerevan (1000m)		NorAmberd (2000m)		Aragats (3200m)	
Type of Secondary particle	Measured count rate	simulated count rate	Measured count rate	simulated count rate	Measured count rate	simulated count rate
Low energy charged particles	8862±108	7202	11593±161	10220	16010±130	17330

Neutral particles	363±19	359	690±27	795	2007±46	1680
High energy muon	4337±67	5477	4473±99	5548	4056±64	8051

4. Response of SEVAN particle detectors to GLEs initiated by the solar protons and neutrons

The arriving from the sun neutrons contains essential information about the ion acceleration, because they are not affected by the magnetic fields. Charged particles, trapping in the interplanetary magnetic usually arrive at the Earth later than gamma rays from solar flares. By observing the neutrons, we can directly probe the energy spectrum of the accelerated ions and also find the production time of the solar particles. Thus measurements of the time series of the solar neutrons and their energy spectra will shed line on operation of the solar accelerators. However, neutron events are very rare and it is not easy to distinguish them from more frequent proton events. The comparison of the count rate enhancements in the layers of the SEVAN module (measured in standard deviations – "sigmas") allows one to distinguish the GLE's originated from solar neutrons incident on terrestrial atmosphere. Table 5 shows that for neutron primaries there is a significant enhancement in the SEVAN thick layer and much less enhancement in thin layer. For proton primaries the situation is vice-versa: the significant enhancement is in the thin layer, and much less in the thick layer.

Table 5. Simulated enhancements (in standard deviations) of the "5-min" count rates corresponding to GLEs initiated by primary neutrons, energy spectrum adopted from Watanabe et al, 2006) and primary protons (Energy spectrum adopted from Zazyan, Chilingarian, 2009).

Detector layer	Solar Protons	Solar Neutrons
Upper 5 cm scintillator	4.8 σ	2.6 σ
Middle 25 cm scintillator	1.7 σ	6.4 σ

5. Forbush decrease events detected by the SEVAN network in the beginning of the 24-th solar activity cycle

The Solar Cycle 24 will peak in May 2013 with a below-average number of sunspots, predicts the panel of experts led by NOAA. Experts predict that Solar Cycle 24 will have a peak sunspot number of 90, the lowest of any cycle since 1928 when Solar Cycle 16 peaked at 78. However, even a below-average cycle is capable of producing severe space weather, all time greatest GLE and geomagnetic storm of 1859 occurred during a solar cycle of about the same size as is

predicted for 2013. Now waiting till Sun accumulates energy for another huge event the SEVAN network detects first Forbush decrease (FD) events. In the middle of February 2011 the active region AR 11158 unleashed 3 solar flares of class M6.6 (13 February, solar coordinates S19, W03), M2.2 (14 February, solar coordinates S20, W14) and strongest X2.2 (15 February, solar coordinates S19, W03S21, W18). All 3 flares were accompanied with CMEs headed to the earth direction. The worldwide network of neutron monitors detects at 18 February sizeable Forbush decrease. The SEVAN network as well detects FD by 3 monitors located in Armenia and by Balkanian monitors located in Zagreb observatory (Croatia) and Mt. Moussala (Bulgaria). The SEVAN module locates in India do not register FD due to large geomagnetic cutoff.

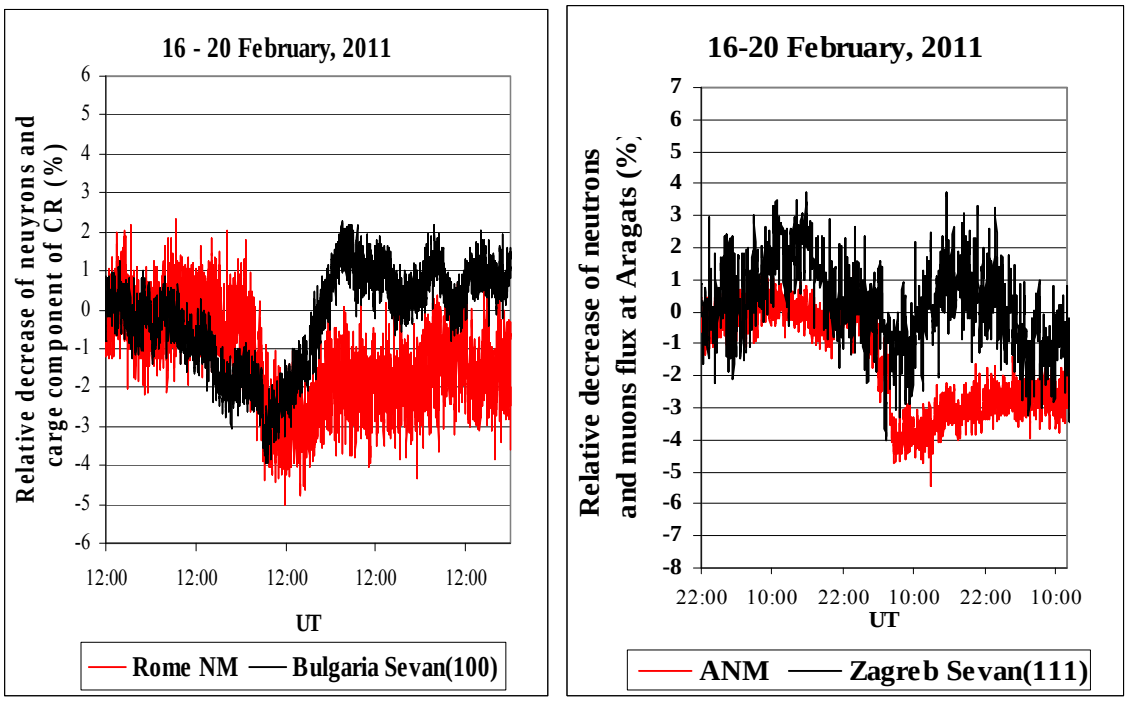

Figure 9. The time profiles of the FD on 18 February, 2011 measured by Zagreb and Moussala SEVAN monitors in comparison with Rome Neutron monitor and Aragats Neutron monitor. The low energy charged particles (combination 100) and high-energy muons (combination 111) are recovering much faster comparing with neutrons measured by Rome and Aragats Neutron monitors.

As we can see in Figure 9 the overall patterns of FD detected in charged particle fluxes are very similar to the ones measured by neutron monitors. However, there are several differences due to location of detectors at different latitudes, longitudes and altitudes. The FD phenomena is global phenomena influenced all globe (may be not the equatorial regions only where the cutoff rigidity is very large); nevertheless the detection of the local differences in time profiles of FD produced by primary particles of different energies is very important and allows to recover the event anisotropy and sometimes also the shape of the ICME. The SEVAN network located on different longitudes (from Zagreb to Delhi) gives possibility to explore FD's shape and the magnitude longitudinal dependence and character of the disturbance and its source (Belov et al., Ruffolo, 1999). The amplitude of FD is dependent on the speed, size, and value of magnetic field of ICMEs (Chilingarian &Bostanjyan, 2010). In this respect registration of FD also in low and high

energy charged particle fluxes can bring additional information for the developing of the model of ICME – magnetosphere interactions.
GCRs are traversing the regions of the disturbed IMF and dependent on their energy are deflected from their path and miss encounter with earth atmosphere. Thus, the disturbed IMF is modulated the GCR flux. As we demonstrate above different components of secondary cosmic rays detected on the earth surface are generated in terrestrial atmosphere by interactions of CRs of various energies; neutrons are generated by protons of lower energies than ones generating electrons; electrons in turn are generated by protons with energies lower than ones generated high energy muons. Therefore, the amplitudes of FDs in neutron, electron and muon fluxes are expected to reflect these energies relations.

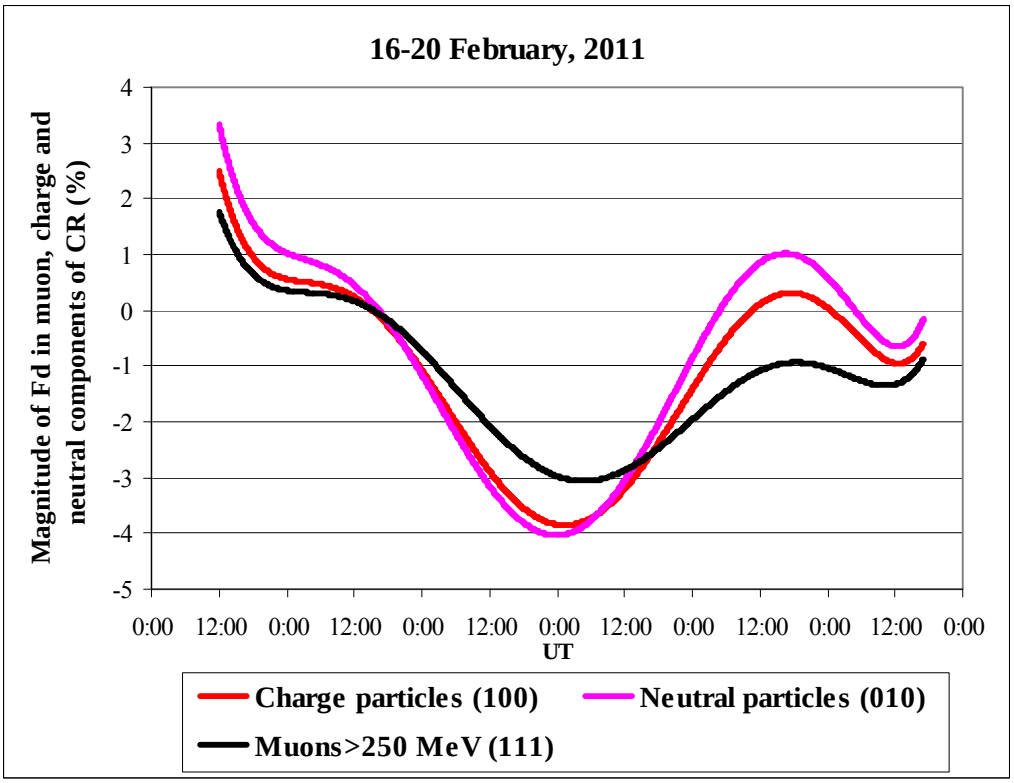

Figure 10. FD as detected by different species of secondary cosmic rays (SEVAN detector combinations).

In the Figure 10 and Table 6 we see that neutral component measured by Aragats SEVAN 010 combination demonstrate 4% decrease practically coinciding with FD measured by the Aragats neutron monitor (4.2%), the low energy charged component (100 combination) ~3.8% decrease and the 111 combination (high energy muons) ~3% decrease. Nor Amberd SEVAN also demonstrated biggest magnitude of FD for the neutral particles; however the magnitude of the low energy charged particles (100) is a bit lower comparing with magnitude of FD measured in the high-energy muon flux. In Zagred magnitudes of FD for all combinations are one and the same. These discrepances signalling necessity of tuning of the measuring channels operation including PM high voltage and shaper thresholds. Thus, the SEVAN detector simulations posted

in the Figures 6-8 and Table 2 are confirmed by the network operation.

Table 6. The magnitudes of FD measured by SEVAN network and Aragats neutron monitor on 18 February.

	Magnitude of FD Aragats, 3200m (%)	Magnitude of FD by Nor Amberd, 2000 m (%)	Magnitude of FD by Zagreb 130m (%)	Magnitude of FD Moussala 2900m (%)	India, New Delhi JNU
SEVAN(100)	-3.8	-2.1	-3	-3	0
SEVAN(010)	-4	-4.2	-3	-	0
SEVAN(111)	-3	-2.3	-3	-	0
Aragats NM	-4.2				

Another solar eruption from active region AR1402 on 23 Jan at 03:38 UT, unleashed a M8.7 flare in associated with full halo CME of 2000 km/s speed reaches earth at 24 January and as we can see in the Figure 11 and Table 7 how the FD was detected by SEVAN modules.

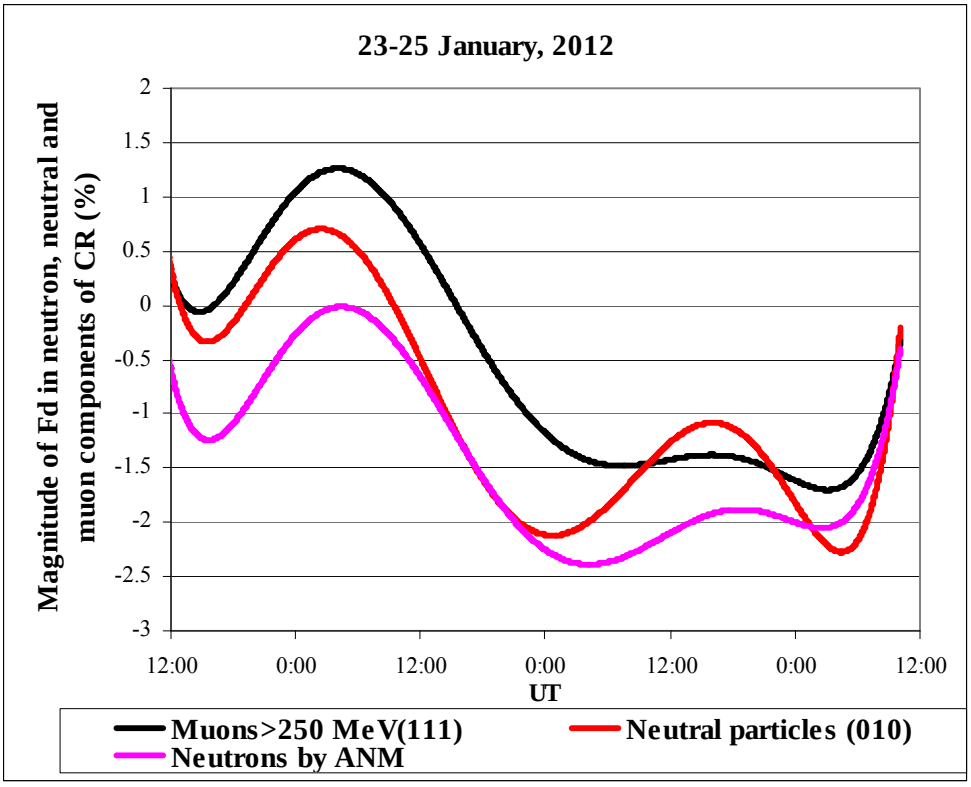

Figure 11. FD of 24 January detected by the Aragats Neutron monitor and SEVAN (010) and 111 combinations.

Table 7.The magnitudes of FD measured by SEVAN network and Aragats neutron monitor on 24 January, 2012.

	Magnitude of FD by Aragats 3200m (%)	Magnitude of FD by Nor Amberd2000m (%)
SEVAN(100)	-1.8	-1.7
SEVAN(010)	-2.1	-3
SEVAN(111)	-1.5	-2
Aragats NM	-2.4	

SEVAN network detects the FDs of 18 February 2011 and 24 January 2012 in the fluxes of neutrons, low energy charged particles and high-energy muons. The patterns of FD in differenct secondary particle species are very similar to ones measured by the NMs only in atmospheric neutron fluxes. However, in addition to neutron monitors SEVAN measures simultaneously FD patterns of other species of secondary cosmic rays giving additional clues for the recovering of the shape and frozen magnetic field of the ICME interacted with magnetosphere.

6.Calculation of the barometric coefficients at the start of the 24th solar activity cycle for SEVAN network

To recover and analyze the solar modulation of the GCRs the influence of the meteorological effects on the flux of the secondary particles reaching the Earth surface should be carefully disentangled. Theory of meteorological effects (Dorman & Dorman, 2005) gives the detailed classification of the metrological effects; it mentioned the barometric one as major influencing particle fluxes. Therefore, it is the greatest importance to accurately measure the barometric coefficients to “unfold” the solar modulation effects. Besides this main goal there exists several independent research problems connected with rigidity, height and solar cycle phase dependence of the barometric coefficient. All these dependences can be investigated by SEVAN network due to different altitudes, various cutoff rigidities and planned long-term operation. At the minimum of solar activity, the GCR flux is enriched by abundant low energy (below 10 GeV) particles, blown out from solar system by intense solar wind at years of maximum of solar activity. Particle detectors located at high latitudes are sensitive to lower primary energies as compared with detectors located at middle – low latitudes, because of lower cutoff rigidity. Detectors located at high altitudes are sensitive to lower primary energies and register more secondary particles than sea level detectors. Detectors registering muons are sensitive to higher energies of primary particles compared with detectors measuring neutrons. Thus, the following relations between barometric coefficients of various particle detectors located in different places and measuring diverse species of secondary CR can be expected:

- Barometric coefficient absolute value for the same secondary particle flux is greater for detectors located at high latitudes as compared with low latitudes;
- Barometric coefficient absolute value for the same secondary particle flux should be greater at minimum of solar activity as compared with maximum;
- Barometric coefficient absolute value for the same secondary particle flux should be greater for high mountain altitudes as compared with lower locations;
- Barometric coefficient absolute value should be larger for neutrons as compared with muons;
- Barometric coefficient absolute value should be larger for low energy muons as compared with high energy muons;
- Barometric coefficient absolute value should be inverse proportional to zenith angle of incident particle flux;
- Barometric coefficient absolute values should be lower for the greater dead times of neutron monitor.

All the mentioned dependences were investigated and discovered during the last 50 years by the networks of neutron monitors and muon detectors (Hatton, 1971). However, due to the peculiarities of detection techniques, scarce statistics, highly different local meteorological conditions, cycle to cycle variations of solar activity the obtained results on the mentioned dependencies are yet more qualitative and additional investigations of the interrelations of barometric coefficients are needed. SEVAN provides ideal platform for such researches. Data for calculation of barometric coefficients of SEVAN modules were selected in 2008, when there were higher than 15 mb continuous changes of atmospheric pressure during the day, and also there were not disturbances of the Interplanetary Magnetic Field (day variations do not exceed 1.5–2 nT). The values of the IMF were obtained from instrument SWEPAM, Advanced Composition Explorer (ACE) spacecraft (http://www.srl.caltech.edu/ACE/ASC/level2/lvl2DATA_MAG.html). The least square method was used to obtain the regression coefficients. Large values of the correlation coefficient prove the correct selection of the reference data. In Table 6 we summarize the calculated barometric coefficients of SEVAN modules. In the columns accordingly are posted the altitude; cutoff rigidity; barometric coefficient; goodness of fit in the form of the correlation coefficient; count rate; relative error; "Poisson" estimate of relative error (standard deviation divides by average count rate).

Table 8. Barometric coefficients, count rates and relative errors of SEVAN units.

Monitor	Altitude (m)	RC (GV)	Barometric coefficient (%/ mb)	Correlation coefficient	Count rate (min)	Relative error	$\frac{1}{\sqrt{N}}$
Aragats SEVAN upper detector	3200	7.1	−0.466 ± 0.018	0.994	20768	0.005	0.0069
Aragats SEVAN middle detector	3200	7.1	−0.406 ± 0.012	0.996	6573	0.011	0.0123
Aragats SEVAN lower detector	3200	7.1	−0.361 ± 0.016	0.992	12481	0.008	0.0089
Nor Amberd SEVAN upper detector	2000	7.1	−0.274 ± 0.016	0.975	9100	0.011	0.0105
Nor Amberd SEVAN middle detector	2000	7.1	−0.342 ± 0.023	0.969	3988	0.015	0.0158
Nor Amberd SEVAN lower detector	2000	7.1	−0.262 ± 0.017	0.973	5103	0.014	0.0141
Yerevan SEVAN upper detector	1000	7.1	−0.251 ± 7.85E−05	0.994	14815	0.008	0.0082
Yerevan SEVAN middle detector	1000	7.1	−0.238 ± 0.014	0.981	3414	0.016	0.0171
Yerevan SEVAN lower detector	1000	7.1	−0.190 ± 0.025	0.903	9505	0.011	0.0102

The values posted in the last two columns should be very close to each other if the Poisson process can describe the particle arrival. Any small deviation manifested the correlation between

detector channels; any large correlation – failures in electronics or data acquisition software (see for details Chilingarian, Hovhannisyan, 2010). In Table 8 and 9 we present barometric coefficients for SEVAN detectors combinations, selecting different species of secondary cosmic rays. Of course, we cannot measure "pure" flux of neutrons, due to the contamination of gamma-quanta and muons. However, as we see from Table 9, events selected as "neutrons" (coincidences 0 1 0 and 0 1 1) demonstrate barometric coefficients approximately twice as events selected as muons.

Table 9. Barometric coefficients, count rates and relative errors of SEVAN monitors for different coincidences.

Monitor	Altitude (m)	RC (GV)	Barometric coefficient (%/ mb)	Correlation coefficient	Count rate (min)	Relative error	$\frac{1}{\sqrt{N}}$
Aragats SEVAN low energy charged particles (coincidence 1 0 0)	3200	7.1	−0.5 ± 0.018	0.995	15389	0.007	0.0080
Aragats SEVAN high energy muons (coincidence 1 1 1 + coincidence 1 0 1)	3200	7.1	−0.351 ± 0.038	0.96	3868	0.014	0.0161
Aragats SEVAN neutral (coincidence 0 1 0)	3200	7.1	−0.511 ± 0.018	0.995	1959	0.019	0.0225
Nor Amberd SEVAN low energy charged particles (coincidence 1 0 0)	2000	7.1	−0.281 ± 0.022	0.957	5941	0.013	0.0129
Nor Amberd SEVAN high energy muons (coincidence 1 1 1 + coincidence 1 0 1)	2000	7.1	−0.242 ± 0.022	0.952	1988	0.026	0.0224
Nor Amberd SEVAN neutrons (coincidence 0 1 0)	2000	7.1	−0.54 ± 0.070	0.899	674	0.037	0.0385
Yerevan SEVAN low energy charged particles (coincidence 1 0 0)	1000	7.1	−0.3 ± 0.014	0.987	9446	0.010	0.0102
Yerevan SEVAN high energy muons (coincidence 1 1 1 + coincidence 1 0 1)	1000	7.1	−0.149 ± 0.035	0.765	4714	0.015	0.0145
Yerevan SEVAN (coincidence 0 1 0)	1000	7.1	−0.4 ± 0.039	0.943	425	0.048	0.0485

7.Investigation of diurnal variations of cosmic rays using SEVAN network

The diurnal variations are the result of complex phenomena involving IMF, magnetosphere and, in addition, dependent on the latitude, longitude and altitude of detector location on the Earth. The diurnal CR variations comprise an important tool for understanding basic physics of the heliosphere and the Earth's magnetosphere. Diurnal variations can be characterized by the

amplitude (maximal value) measured in daily time series and by phase (time of the maximal amplitude). Different species of the secondary CR undergo different diurnal variations. It is obvious that more the most probable primary energy of the monitored CR species – less should be the amplitude of diurnal variation. Therefore, the third parameter, characterizing the diurnal variations at definite location and time, is so called upper limiting rigidity, i.e., the threshold rigidity not influenced by the solar, interplanetary and geomagnetic disturbances. The detailed investigation of the diurnal variations can comprise a basis of scientific data to be used in a wide context of solar-terrestrial connections. In this section we present measurements of the phase, amplitude for the SEVAN monitors at the minimum of the solar activity year. This data will be used for physical analysis of SEVAN particle detectors data as 24th solar activity cycle proceeds.

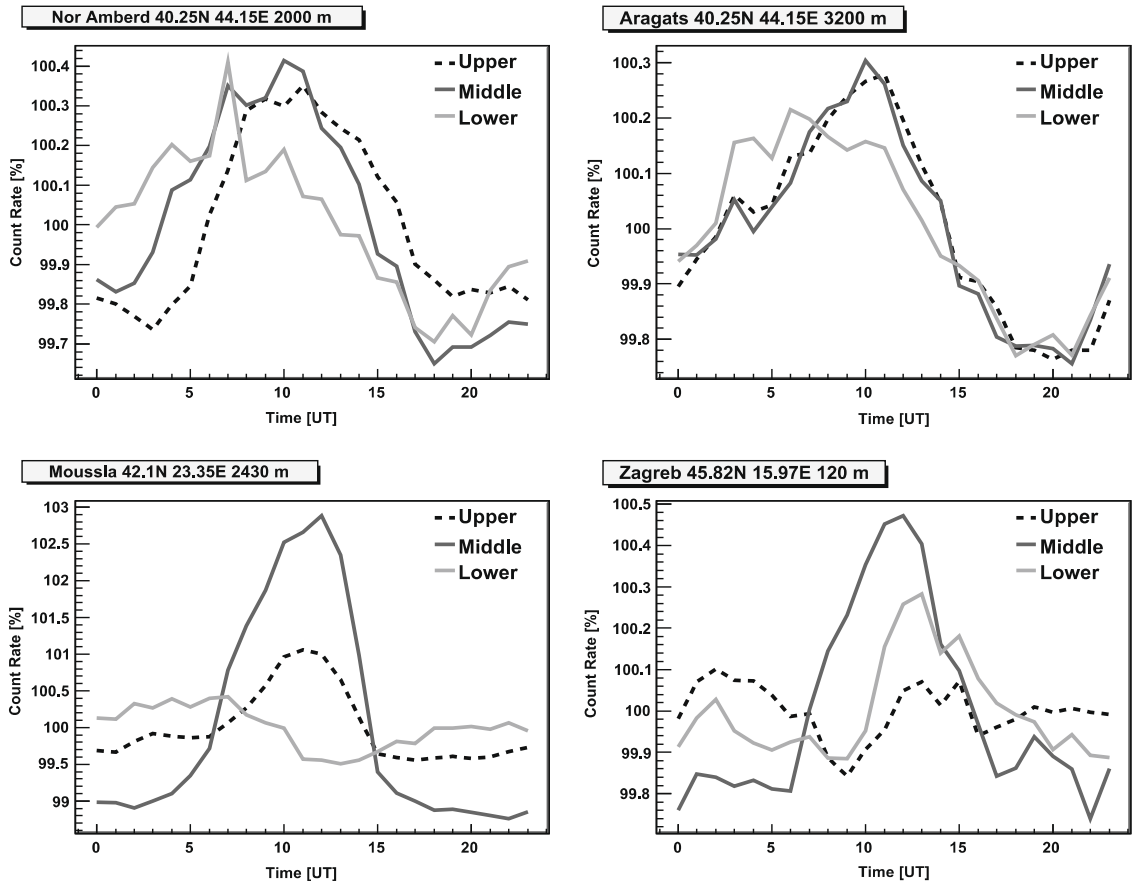

Figure12. Daily variations of high, low energy charged fluxes and neutral fluxes according to the SEVAN detectors located in Nor Amberd, Aragats, Moussala and Zagreb. Month-averaged daily count rates of Nor Amberd May 2008 data, Aragats – October 2008, Moussala and Zagreb December 2008–January 2009.

In Figure12 we can see that detectors located at close geographic co-ordinates demonstrate similar patterns of the daily variations. When comparing Aragats and Balkanian monitors we can deduce that both latitude and longitude of site location influence the diurnal variations' pattern.

However, very large amplitude of Moussala monitor's middle scintillator point on possible defects in light proofing of the middle detector. Filtered and pressure corrected (Chilingarian and Karapetyan, 2011) daily data from Figure 12 were fitted by the harmonic approximation function for each day of the selected period. In this way, distributions of amplitudes and phases of daily variation were got. The following approximation was used (Kudela et al., 2008):

$$f(t_i) = A + B \cdot \cos(\omega t_i + \psi) \qquad (1)$$

Here A is the daily average value of cosmic ray intensity, B is the amplitude of daily variations, ω is the angular frequency and ψ is the phase of daily variations. The quality of fit d, the difference between experimental data and the fit is calculated according to Kudela et al. (2008):

$$d^2 = \sum_{i=1}^{n} d_i^2 = \sum_{i=1}^{n} [Y_i - f(t_i)]^2 \qquad (2)$$

Amplitudes and phases obtained from Eq. (1), and fit quality calculated by Eq. (2) are presented in Table 10. We do not fit curves with two peaks and without apparent peak. For Nor Amberd's SEVAN daily changes are bigger for the middle layer (lower energy primaries). In local times the maximums are at 15:00 for upper and middle detectors, and few hours earlier for lower detector. Aragats' upper and middle detectors also show maximum with magnitude about 0.2% at 15:00 LT, and lower detectors show variations approximately 0.2% at 11:00 LT. For these two monitors, secondary particles corresponding to higher energy primaries show smaller variations.

Table 10 .Daily variations of the SEVAN data; Nor Amberd data of May 2008, Aragats data of October 2008, Moussala and Zagreb data of December 2008–January 2009.

	Median amplitude (%)	Median phase (local time)	Quality of the fit	Most probable primary energies (GV)
SEVAN NA upper detector	0.28	15:13	1.33	14.6
SEVAN NA middle detector	0.34	12:55	1.15	7.1
SEVAN NA lower detector	0.24	10:36	0.18	18.4
SEVAN Aragats upper detector	0.23	12:42	0.71	14.6
SEVAN Aragats middle detector	0.21	12:27	0.62	7.1
SEVAN Aragats lower detector	0.20	11:17	0.33	18.4
SEVAN Mousalla upper detector	0.55	11:58	2.31	

SEVAN Mousalla middle detector	1.80	12:33	8.16	
SEVAN Mousalla lower detector	No peaks			
SEVAN Zagreb upper detector	Two peaks			
SEVAN Zagreb middle detector	0.28	12:39	1.35	
SEVAN Zagreb lower detector	0.12	14:43	0.51	

The first data available from SEVAN network demonstrate that charged component variations are comparable with neutron variation and that diurnal variations are sensitive to longitude of site location.

8. Thunderstorm Ground Enhancements (TGE) detected by SEVAN

Facilities of the Aragats Space Environment Center (ASEC) (Chilingarian et al, 2003, 2005) observe charged and neutral fluxes of secondary cosmic rays by the variety of particle detectors located in Yerevan and on slopes of Mt. Aragats at altitudes 800, 2000 and 3200 m. ASEC detectors measure particle fluxes with different energy thresholds as well as EAS initiated by primary proton or stripped nuclei with energies greater than 50– 100 TeV (Chilingarian et al., 2010). Detection of abrupt enhancements of the particle detector count rates correlated with thunderstorm activity, so called Thunderstorm Ground Enhancements (TGEs) detected during 2008-2011 years brings vast amount (343 TGE events) of small and very few large TGEs (only 6 TGE events with amplitude exceeding 20%) allowing the detailed analyses and taxonomy of new high-energy phenomena in atmosphere. Small TGEs can be explained by the modification of the energy spectra of charged particles in the electrical field of thunderclouds. Due to asymmetry of positive-to-negative flux of secondary cosmic rays in terrestrial atmosphere, peaks and deeps can arise in time series of count rates of surface particle detectors. These effects have been theoretically analyzed in (Dorman and Dorman, 2005). Measurements at ASEC and simulation with GEANT4 package confirm additional flux of gamma rays up to 1000% in the energy range 1-10 MeV and up to 5% in the energy range up to 100 MeV. Simultaneously deeps in the muon flux at energies above 200 MeV was obtained by simulations and detected by SEVAN detectors, 101 and 111 combinations. Electrical field meters (Boltek firm electrical mill EFM100, http://www.boltek.com/efm100.html) and lightning detectors (StormTracker Lightning Detection System powered by the software from Astrogenic systems, http://www.boltek.com/stormtracker) installed at Aragats allow correlating the measured particle fluxes with electrical field disturbances and with occurrences of lightning of different types. The electrical mill was calibrated by fair weather electrical field according to firm instructions. In database of SEVAN time series we can find significant non-random variations of cosmic ray intensity in absence of any lightning occurrences, signaling that the electrical field strength in the cloud is below the RREA threshold. Electrons and negative muons are accelerated downwards by lower dipole before reaching particle detector. The positrons and positive muons as well as protons will be decelerated in the lower dipole. The positive charge of primary cosmic rays (mostly protons and stripped nuclei) introduces several asymmetries between particles and antiparticles born in

atmospheric cascades. The intensity of the MeV electrons is larger than intensity of positrons of the same energies in energy range 1-50 MeV; the intensity of positive muons above 100 MeV is larger comparing with intensity of the negative muons, see Figure 13 and 14.

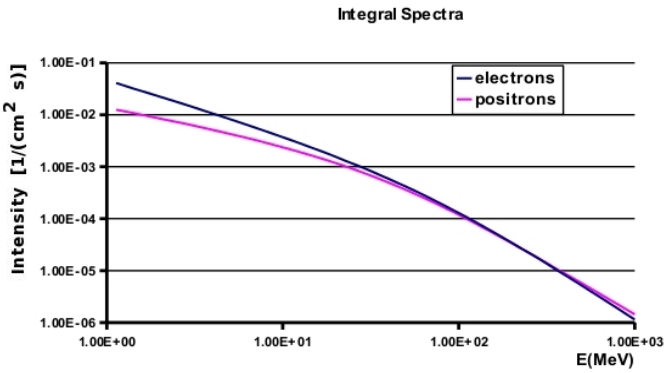

Figure 13.**Energy spectra of electrons and positrons at altitude of 5000 m a.s.l.**

We can see in the Figure13 that the number of electrons with energies below 50 MeV at 5000 m altitudes is significantly larger comparing with positrons. It means that positive electrical field in the thundercloud will significantly alter the total intensity of charged particles of low energy registered by scintillators at the Earth surface. The changes of intensity will manifest themselves as peaks and deeps in the time series of count rates of particles registered by the scintillators located on the Earth surface. The energy spectrum of electrons will be shifted to the right (mean energy becoming larger) leading to the additional bremsstrahlung gamma rays; shifting to the left energy spectrum of positrons cannot compensate these enhancements because of their shortage. The attenuation length of the electrons in the energy range of 1-100 MeV is much less comparing with the one of the gamma rays. Therefore, most of TGE events are detected in the fluxes of gamma rays born by accelerated cosmic ray electrons.

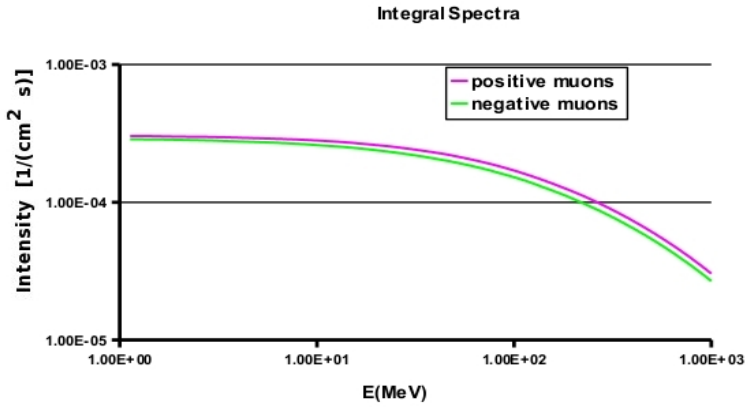

Figure 14.**Energy spectra of muons at altitude 5000 m a.s.l**

Interestingly, positive fields have opposite influence on counts of muons at energies above 200 MeV. Among ASEC particle detectors there are scintillators with energy threshold greater than 200 MeV and the electron acceleration described above will not influence their count rate. Due to abundance of positive muons over negative (1.3 -1.4 times at 100-500 MeV energies, see Figure 14) the braking of positive muons in the positive electrical field cannot be compensated by the acceleration of the negative muons in the same field. The consequences of this asymmetry you can see in the Figure15: on October 4, 2010 we detected ~6% deficit in the flux muons with energies greater than ~250 MeV, simultaneously detecting huge excess of low energy gamma rays and electrons. Observational data of the Aragats station's monitors obtained during 2008-2011, when solar activity was minimal and corresponding solar modulation effects were absent, demonstrates several remarkable TGE events; few of them were accompanied by the muon flux decrease. In Figure 16 one can see the count rates of the SEVAN detector on 4 October 2010. The threshold of the upper detector due the matter of the roof above is ~ 15MeV; it counts exhibits a large peak lasting ~10 minutes with maximal counting rate at 18:23. This peak is due to penetrated gamma rays (and small portion of electrons) of the Relativistic runaway electron avalanche (RREA, Gurevich et al., 1992, Babich et al., 1998, Dwyer, 2007, Khaerdinov et al., 2005) process in the thundercloud just above the building where detector is located (Chilingarian et al., 2011). For the same minutes the channels 111 shows pronounced decrease. Energy of particle necessary to penetrate lead filters and be detected in all three layers (combination 111) is ~250MeV.

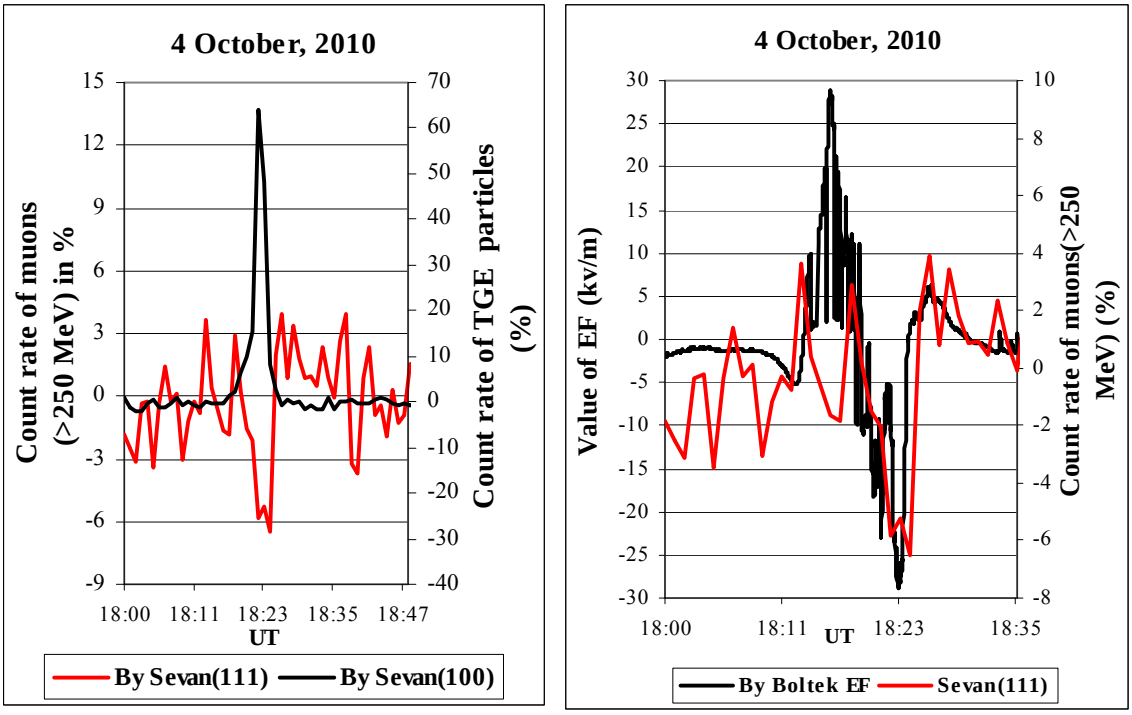

Figure 15. The count rates of SEVAN 100 and 111 combinations along with the changing near surface electrical field. The positive field in the thundercloud (electrons are accelerated downwards) is stopping positive muons; charge ratio of positive-to-negative muons is (~1.3), therefore we detect ~6% deficit of the flux of high-energy muons (energy > 250 MeV); simultaneously huge TGE in gamma ray and electron fluxes was measured.

Both increase of the RREA electron and gamma ray fluxes occur during negative near-ground electrical field. According to our model, (see Figure 10 of Chilingarian et al, 2011) TGE event started with formation in the bottom of the cloud of the lower positive charged region (LCPR). LCPR with main middle negative charged layer compose the lower dipole accelerated electrons downward. The lower dipole is responsible for RREA process that leads to large TGEs. Unfortunately, we cannot yet perform calculations according to our model of TGE/RREA because the electrical field within lower dipole is very difficult to measure. Surprisingly the SEVAN module gives us possibility to estimate this field at least roughly. Observed deficit ~6% is caused mostly by the positive muons, which spectrum is affected significantly by the positive potential of the thundercloud. Therefore, by deriving the relationship between the measured deficit and unknown electric potential in the cloud it will be possible to estimate the electrical potential within cloud, based on observed values of high-energy muon deficit.

The huge flux of the gamma rays measure at 18:23 on 4 October, 2010 was used to check the Aragats SEVAN ability to detect gamma ray flux by 010 the combination. Simulating the passage of the recovered gamma-ray flux through the roof above and detector and taking into account the detector response to gamma rays and electrons, we have estimated the expected

number of gamma rays detected by the “010” combination to be 1459 respectively. This value is in a good agreement with experimentally measured value of 1452 ± 42.

In Figure 16 we post the pattern of the first TGE detected in Yerevan (800 m a.s.l.) at midnight July 18, 2011. Again during thunderstorm negative near surface electrical field was measured, although not so large as on Aragats. At the same time upper layer of Yerevan SEVAN module, located on the roof of CRD headquarters registered significant peak of ~6% (~ 7 standard deviations). With high probability it was gamma rays, though electron TGE flux should attenuate reaching the detector. The thunderclouds above Yerevan are rather high and electrons will attenuate in dense air.

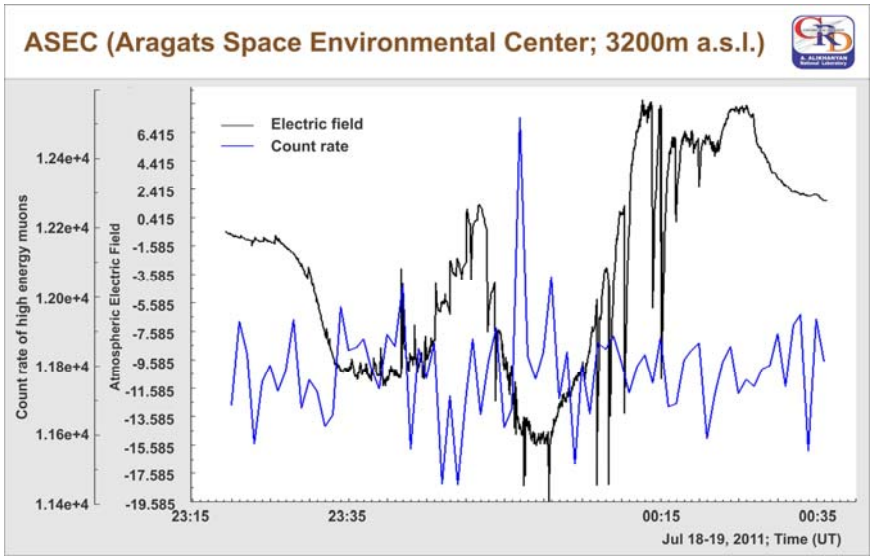

Figure 16. The first TGE registered by Yerevan SEVAN.

9. Conclusion

Reliable forecasts of major geomagnetic and radiation storms are of great importance because of associated Space Weather conditions leading to failures of space and earth surface based technologies as well as posing radiation hazards on crew and passengers of satellites and aircraft. Measurements of Solar Wind parameters performed at spacecraft located at L1 provide too short a time span for mitigation actions to be taken. Networks of particle detectors located at the Earth’s surface provide another piece of valuable information on major storms.

Networks of particle detectors on Earth’s surface provide timely information and constitute an important element of planetary Space Weather warning services. The big advantage of ground based particle detectors is their consistency, 24 h coverage, and multi- year operation. In contrast the planned life of the satellites and spacecraft is only a few years, they are affected by the same solar blast that they should alert, and space-born facilities instead of sending warnings are usually set in the stand-by mode.

The multi-particle detectors proposed in the present paper will probe different populations of primary cosmic rays. The basic detector of the SEVAN network is designed to measure fluxes of neutrons and gammas, of low energy charged particles and high-energy muons. The rich information obtained from the SEVAN network located mostly at low and middle latitudes will allow estimating the energy spectra of the highest energy SCR. The SEVAN network will be sensitive to very weak fluxes of SCR above 10 GeV, a very poorly explored region of the highest energy. To understand the sensitivity of the new type of particle detectors to high-energy solar ions we investigate the response of SEVAN basic units to galactic and solar protons. The hard spectra of solar ions at highest energies (γ = -4 to - 5 at rigidities >5 GV) indicate the upcoming very intense solar ion flux with rigidities >50 MV, very dangerous for satellite electronics and astronauts. The SEVAN network detectors will also allow distinguishing very rare and very important GLEs initiated by primary neutrons.

Summarizing, the hybrid particle detectors, measuring neutral and charged fluxes provide the following advantages over existing detector networks measuring single species of secondary cosmic rays:

- Enlarged statistical accuracy of measurements;
- Probe different populations of primary cosmic rays with rigidities from 3 GV up to 20–30 GV;
- Reconstruct SCR spectra and determine position of the spectral ‘‘knees’’;
- Classify GLEs in ‘‘neutron’’ or ‘‘proton’’ initiated events;
- Gives possibilities to investigate energy dependences of the barometric coefficients and diurnal wave;
- Estimate and analyze correlation matrices among different fluxes;
- Significantly enlarge the reliability of Space Weather alerts due to detection of three particle fluxes instead of only one in existing neutron monitor and muon telescope world-wide networks;

The phenomenon of decreasing of the high-energy muon flux measured by SEVAN detector during TGEs can be explained by the shifting of energetic spectrums of muons in electric field. During positive flux in the lower dipole that accelerates electrons and negative muons downwards spectrum of negative muons shifts right, whereas spectrum of positive muons shift left on the amount corresponding to net potential difference of electrical field. In the result of such shifting the fluxes of muons above threshold energy of detector are changed: flux of negative muons increases, while the flux of positive muons decreases. Summary the total particle’s flux decreases (SEVAN cannot distinguish positive and negative muons) because number of positive muons is greater (~30% at energies above 100 MeV) than number of negative muons. By the measured deeps in high energy muon time series it is

possible to remotely estimate the total potential drop in thundercloud; the problem that escaping the solution till now-the-days because of absence of adequate techniques.

Acknowledgement

Our work was supported by IHY-2007 initiative, and we thank H.Haubold, J.Davila, N. Gopalswami for being so instrumental in creating worldwide instruments networks. Our work was supported by ISTC A1554 grant and EOARD grant FA 8655-07-01-3014. Authors thanks SEVAN instrument hosts D. Rosa, J. Stamenov, K. Kudela, S. Mukherjee for their interest to be a part of SEVAN network and for operating SEVAN modules.

Reference:

L. P. Babich, E. N. Donskoi, I. M. Kutsyk, and Kudryavtsev, Phys. Lett. A 245, 460 (1998).

A.V. Belov, L.I.Dorman, E.A. Eroshenko, N.Iucci, G. Villoresi, V.G. Yanke. Search forPredictors of Forbush Decreases., Proc. 24th Inter. Cosmic Ray Conf, 4, 888-891, 1995.

Bostanjyan, N., Chilingaryan A., Eganov V., Karapetyan g., On the production of higest energy solar protons on 20 January 2005. Adv. Space res. 39, 1454-1457, 2007.

M. Boezio, V. Bonvicini, P. Schiavon, A. Vacchi, et al., Astropart. Phys. 19 (2003) 583–604.

A. Chilingarian and A. Reymers, Investigations of the response of hybrid particle detectors for the Space Environmental Viewing and Analysis Network (SEVAN), Ann. Geophys, 26, (249-257), 2008.

A. Chilingarian, N. Bostanjyan On the relation of the Forbush decreases detected by ASEC monitors during the 23rd solar activity cycle with ICME parameters.Advances in Space Research 45 (2010) 614–621.

A. Chilingarian, G. Hovsepyan, K., et al., Space Environmental Viewing and Analysis Network (SEVAN), Earth, Moon and Planets: Vol.104, Issue 1, (195), 2009.

Chilingarian, A.Daryan, K.Arakelyan, et al., Ground-based observations of thunderstorm-correlated fluxes of high-energy electrons, gamma rays, and neutrons, Phys.Rev. D., 82, p. 043009, 2010.

Chilingarian, G. Hovsepyan, and A. Hovhannisyan, Particle bursts from thunderclouds: Natural particle accelerators above our heads, Physical review D 83, p. 062001, 2011.

S. Chilingaryan et al, Journal of Physics: Conference Series, Volume 219, Part 4, 2010.

Hatton C. J., Progress in Elementary Particles and Cosmic Ray Physics, 10, 1- 100, North Holland, 1971

Dorman L. I. and Dorman I. V., Advances in Space Research, Volume 35, pp 476-483, 2005.

J. R. Dwyer, Phys. Plasmas 14, 042901 (2007).

A. V. Gurevich, G. M. Milikh, and R. A. Roussel-Dupre, Phys. Lett. A 165, 463 (1992).

D. Heck, J. Knapp, A Monte Carlo Code to Simulate Extensive Air Showers, ForschungszentrumKarlsryhe, FZKA Report 6019, 1998.

Haurwitz et al., 1965 M.W. Haurwitz, S. Yoshida and S.I. Akasofu, Interplanetary magnetic field asymmetries and their effects on polar cap absorption effects and Forbushdecreases. J. Geophys. Res., 70 (1965), pp. 2977–2988

EXPACS **(**http://phits.jaea.go.jp/expacs/

N. S. Khaerdinov, A. S. Lidvansky, and V. B. Atmos. Res. 76, 346 (2005).

Kudela, K., Firoz, K.A., Langer, R., et al. On diurnal variation of cosmic rays: statistical study of neutron monitor data including LominskyŜtit, in: Proceedings of 21st ECRS-2008. Available from: <http://www.ecrs2008.saske.sk/dvd/s4.15.pdf>, 2008.

Kuwabara, T., et al. (2006), Realtime cosmic ray monitoring system for space weather, Space Weather, 4, S08001, doi:10.1029/2005SW000204.

K. Leerungnavarat, D. Ruffolo, J.W. Bieber, Astrophys. J. 593 (2003) 587–596.

Munakata, K., J. W. Bieber, S. Yasue, C. Kato, M. Koyama, S. Akahane, K. Fujimoto, Z. Fujii, J. E. Humble, and M. L. Duldig (2000), Precursors of geomagnetic storms observed by the muon detector network, J. Geophys.Res., 105(A12), 27,457–27,468, doi:10.1029/2000JA000064.

M. Rockenbach A. Dal Lago, W. D. Gonzalez, et.al.,eomagnetic storm's precursors observed from 2001 to 2007 with the Global Muon Detector Network (GMDN), J. Geophys.Res., 38, L16108, doi:10.1029/2011GL048556, 2011.

D. Roša, Ch. Angelov, K. Arakelyan, et al., Sevan CRO particle detector for solar physics and space weather research, Cent. Eur. Astrophys. Bull. 34, 115–122, 2010.

D. Ruffolo,J.W.Bieber, P.Evenson, and R. pile., Precursors to Forbush Decreases and Space Weather Prediction., Proceedings of the 26th International Cosmic Ray Conference. August 17-25, 1999. Salt Lake City, Utah, USA.

Watanabe, K., Gros, M., Stoker, P. H., et al.: Solar neutron events of2003 October November, Astrophys. J., 636, 1135–1144, 2006.

Zazyan, M., Chilingarian, A. Calculations of the sensitivity of the particle detectors of ASEC and SEVAN networks to galactic and solar cosmic rays. Astropart. Phys. 32, 185–192, doi:10.1016/j.astropartphys.2009. 08.001, 2009.

Zhang J.L., Tan Y.H., Wang H., et al., The YangbajingMuon–Neutron Telescope, NIMA, 623, 1030-1034, 2010, doi:10.1016/j.nima2010.08.091.